Properties of Nucleon Resonances by means of a Genetic Algorithm

C. Fernández-Ramírez,[1,*] E. Moya de Guerra,[2,3] A. Udías,[4] and J.M. Udías[2,†]

[1] *Center for Theoretical Physics, Laboratory for Nuclear Science and Department of Physics, Massachusetts Institute of Technology, 77 Massachusetts Ave., Cambridge, MA 02139, USA*

[2] *Grupo de Física Nuclear, Departamento de Física Atómica, Molecular y Nuclear, Facultad de Ciencias Físicas, Universidad Complutense de Madrid, Avda. Complutense s/n, E-28040 Madrid, Spain*

[3] *Instituto de Estructura de la Materia, CSIC, Serrano 123, E-28006 Madrid, Spain*

[4] *Departamento de Estadística e Investigación Operativa, Escuela Superior de Ciencias Experimentales y Tecnología, Universidad Rey Juan Carlos, Camino del Molino s/n, E-28943 Fuenlabrada, Spain*

(Dated: June 24, 2008)

We present an optimization scheme that employs a Genetic Algorithm (GA) to determine the properties of low-lying nucleon excitations within a realistic photo-pion production model based upon an effective Lagrangian. We show that with this modern optimization technique it is possible to reliably assess the parameters of the resonances and the associated error bars as well as to identify weaknesses in the models. To illustrate the problems the optimization process may encounter, we provide results obtained for the nucleon resonances $\Delta(1230)$ and $\Delta(1700)$. The former can be easily isolated and thus has been studied in depth, while the latter is not as well known experimentally.

PACS numbers: 14.20.Gk, 13.60.Le, 02.60.Pn, 02.70.-c

arXiv:0805.4178v2 [nucl-th] 24 Jun 2008

I. INTRODUCTION

In recent years, in order to study the properties of low-lying nucleon resonances and assess their parameters (masses, widths, and electromagnetic coupling constants), significant experimental and theoretical efforts have been devoted to the process of meson production from the nucleon, which is achieved by exciting the nucleon resonances by means of photonic or electronic probes, and to the study of the decays of these resonances into mesons (mainly pions) [1]. The parameters of these resonances, predicted by several theoretical models of baryons – lattice Quantum Chromodynamics [2], Skyrme models [3], quark models [4] – can be compared to the ones extracted from experimental data, which usually requires the aid of reaction models. This process of extracting the nucleon excitations parameters from experimental data is thus a crucial requirement in order to validate different hadron models, as it provides a guide for improving hadron models and for identifying the most reliable ones [5]. Together with pion scattering off the nucleon, single pion photoproduction is the most suitable process for studying the low-lying baryon spectrum. In fact, in recent years the experimental database [6] has increased considerably and many experimental programs have been run at different facilities such as LEGS (Brookhaven) [7] and MAMI (Mainz) [8].

The extraction of the parameters of the resonances by means of a comparison of the results of reaction models to experimental data is an excellent example of a highly involved optimization task. Problems in which a set of parameters must be established through comparison with experimental data are ubiquitous in physics. Often, optimization has been considered a minor topic (at times even trivial) by the particle and nuclear physics community which has relied on gradient-based optimization tools such as MINUIT [10]. Sometimes, however, optimization problems are very complicated and gradient-based routines alone are not sufficient for the purpose, because the function to fit presents a complex structure with many local optima in which the codes get trapped before reaching anywhere near the desired absolute optimum. Thus, until relatively recently, fitting model parameters to data has been a kind of art. This was particularly the case when thousands of data needed to be compared to the results of sophisticated models that depended on more than just a few parameters. In such cases, many instances of the optimization procedure have to be repeated, after manually adjusting the parameters, and specific care must be taken to prevent the optimization procedure from getting stuck at the many possible local minima positions.

Recently, in nuclear and particle physics, more credit is being given to modern optimization procedures [11, 12, 13, 14, 15, 16] and to error estimations on the parameters stemming from the fits. Modern and sophisticated optimization techniques such as simulated annealing [17] and genetic algorithms (GA) [18] have been developed over the last twenty years and have been applied to problems which are impossible to tackle with conventional tools.

In this paper we present a hybrid optimization procedure which combines a GA with a gradient-based ("hill-climbing") routine `E04FCF` from the NAG library [9]. The GA performs the bulk of the optimization efforts, ensuring that the parameter space is fully surveyed and lo-

*Electronic address: cefera@mit.edu
†Electronic address: jose@nuc2.fis.ucm.es

cal minima are avoided, while the conventional gradient-based routine, when applied to the preliminary minima found by the GA, provides fine-tuning and speeds up convergence. We have applied this tool to a complex, multi-parametric optimization problem, namely the determination of nucleon resonances parameters by comparing the results of a realistic model for the photo-pion production reaction to data. As a by-product, the optimization procedure provides insight into the reliability of the values (error bars) of the parameters extracted and information on their physical significance.

This paper is organized as follows: in Section II we briefly present the model for pion photoproduction on free nucleons from threshold up to 1.2 GeV developed in Refs. [13, 14, 15]. In Section III we present the strategy applied to solve the problem. In Section IV we present the GA in detail. In Section V we show the results obtained by the algorithm, analyze its performance and comment on the error bar estimates and the physical significance of the parameters extracted. Finally, in Section VI we present our conclusions.

II. THE REACTION MODEL

The reaction model is based upon a phenomenological Lagrangian and it allows us to isolate the contribution of the resonances, calculate their bare properties, and compare these properties with the values provided by nucleonic models [13, 19]. In addition to Born terms (those which involve only photons, nucleons and pions) and vector-meson exchange terms (ρ and ω), the model includes all four star resonances quoted in the Particle Data Group (PDG) [20] up to 1.8 GeV of mass and up to spin-3/2: $\Delta(1232)$, N(1440), N(1520), $\Delta(1620)$, N(1650), $\Delta(1700)$, and N(1720). The internal structure of the nucleonic excitations shows up in the values of the electromagnetic coupling constants that appear in the Lagrangian. The model displays chiral symmetry, gauge invariance, and crossing symmetry, and incorporates a consistent treatment of the interaction with spin-3/2 particles that avoids well-known pathologies of previous models [13, 14, 21]. Furthermore, the dressing of the resonances is considered by means of a phenomenological width which takes into account decays into one and two π's and one η. This width is included in a way that fulfils crossing symmetry and thus it contributes to both the direct and crossed channels of the resonances. We assume that the final state interactions (FSI) in the πN rescattering factorize and can be included through the distortion of the πN final state wave function. We include this distortion in a phenomenological way by incorporating a phase $\delta_{\rm FSI}$ to the electromagnetic multipoles. We fix this phase so that the total phase of the electromagnetic multipole is identical to that of the energy dependent solution of SAID [6]. In this way, we disentangle the parameters of the electromagnetic vertex from the FSI effects.

III. MINIMIZATION STRATEGY

Our minimization procedure follows the one in [12] although we use a more sophisticated GA and employ the `E04FCF` routine from the NAG library [9] instead of `MINUIT` [10] code. We apply the minimization scheme to a realistic meson production model and the aim of our minimization is different. While in [12] the aim was to establish the existence of certain resonances, in this paper our goal is to determine the parameters of well-established nucleon resonances and to obtain estimates on the reliability of these parameters and their associated error bars.

The function to minimize is the χ^2 defined by

$$\chi^2 = \sum_j \frac{\left(\mathcal{M}_j^{exp} - \mathcal{M}_j^{th}\left(\lambda_1, \ldots, \lambda_n\right)\right)^2}{\left(\Delta\mathcal{M}_j^{exp}\right)^2}, \qquad (1)$$

where $\mathcal{M}^{exp}$ stands for the current energy independent extraction of the multipole analysis of SAID up to 1.2 GeV for E_{0+}, M_{1-}, E_{1+}, M_{1+}, E_{2-}, and M_{2-} multipoles in the three isospin channels $I = \frac{3}{2}, p, n$ for the $\gamma p \to \pi^0 p$ process [6]. $\Delta\mathcal{M}^{exp}$ is the experimental error and $\mathcal{M}^{th}$ is the multipole value given by the model. It depends on parameters λ_1, ...,λ_n. We have taken into account 1,880 data for the real part of the multipoles and the same amount for the imaginary part. Thus, 3,760 data points have been used in the fits. Unlike cross-sections or asymmetries, electromagnetic multipoles are not directly measured quantities and some elaboration of the raw experimental data is needed to obtain these multipoles. However, we have chosen, as it is very often done in this field, to fit electromagnetic multipoles instead of other observables. Several reasons are mentioned when fitting to multipoles. On one hand, electromagnetic multipoles are more sensitive to coupling properties than other observables, so deficiencies in the model may show up more clearly. The second reason is that, in principle, all the observables can be expressed in terms of multipoles. Thus, if the multipoles are properly fitted by the model, so should be other observables.

In order to determine the resonance parameters that best fit the data, we have written a hybrid optimization code based on a GA combined with the `E04FCF` routine from the NAG library [9]. Although GA, are computationally more expensive than other algorithms, in a minimization problem it is much less likely for them to get stuck at local minima than it is for other methods, namely gradient-based minimization methods. GAs allow us to explore a large parameter space more efficiently. Thus, in a multi-parameter minimization such as the one we face here, they are probably a very efficient way of searching for the best minimum. In the next section we will go through the details of the GA.

The parameters for the model (λ_j) are divided into two different kinds: (i) Those that are obtained from models or experiments other than pion photoproduction, namely vector-meson coupling constants (three parameters) and

masses and widths of the nucleon resonances (fourteen parameters, one mass and one width for each resonance which have been taken from [22]), and (ii) those that are extracted from pion photoproduction data, namely electromagnetic coupling constants (fifteen parameters) and the cutoff Λ for Born terms and vector-meson exchanges. We have allowed the algorithm to vary all the parameters (see Tables I and II). However, the parameters in the first group have been varied within a very small range, the experimentally allowed values for the vector-meson coupling constants and ± 2 MeV for the masses and widths of the nucleon resonances. The reason for allowing these parameters to vary, even though the range of variation is minimal, is to make room for the algorithm to search for the global minimum and to take into account the error bars for these parameters into the possible solution. This should help to prevent the algorithm for being trapped in local minima.

The variation range for the second group of parameters are chosen to explore a large region of parameter space. Hence we avoid introducing prejudgments on their values based on previous analysis. We prefer to use the helicity amplitudes (for their definition and connection with coupling constants see Refs. [13, 14, 20]) to define the ranges, instead of the electromagnetic coupling constants. We allow them to vary in the range $[-1, 1]$ GeV$^{-1/2}$.

The cut-off Λ is included in the form factors that multiply the Born terms and vector-meson exchange invariant amplitudes. We use the form factors suggested in [23], which respect gauge invariance and crossing symmetry. For these Born terms

$$\begin{aligned}\hat{F}_B(s,u,t) =& F(s) + F(u) + G(t) - F(s)F(u) \\ & - F(s)G(t) - F(u)G(t) + F(s)F(u)G(t),\end{aligned} \tag{2}$$

where

$$F(l) = \left[1 + \left(l - M^2\right)^2 / \Lambda^4\right]^{-1}, \quad l = s, u; \tag{3}$$

$$G(t) = \left[1 + \left(t - m_\pi^2\right)^2 / \Lambda^4\right]^{-1}. \tag{4}$$

and s, u, and t are the Mandelstam variables. For vector mesons, we adopt $\hat{F}_V(t) = G(t)$ with the change $m_\pi \to m_V$. To reduce the number of free parameters for the model we use the same Λ for both vector mesons and Born terms.

The form factors take non-resolved structure effects and higher order terms in the scattering matrix expansion into account. Thus, the cut-off Λ is related to the energy scale of the effective theory and the sensible values for Λ should be of the order of the nucleon mass (actually, in our best fit we obtain $\Lambda = 0.943$ MeV). For this reason, in the minimization process, we restrict Λ to the range $[0.1, 2.0]$ GeV.

In order to perform the minimization, the range of variation of each parameter is mapped into the $[0, 1]$ interval for the GA and into $(-\infty, +\infty)$ for the `E04FCF` routine. This latter step is done by means of the transformation

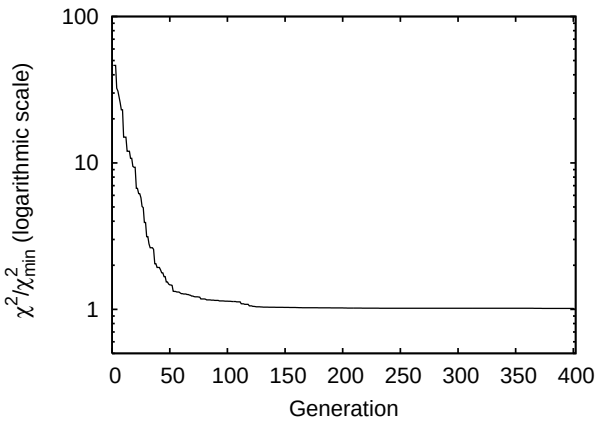

FIG. 1: Example of the evolution for a champion in one run of the GA. For the first generations (up to generation 40 or 50) evolution is driven by crossover. After this, small improvements are seen due to mutations.

$$x_j = \arcsin\left[\frac{\lambda_j - \lambda_j^{max}}{\lambda_j^{max} - \lambda_j^{min} - 1}\right], \tag{5}$$

where λ_j is the model parameter, x_j is the mapping of λ_j into $(-\infty, +\infty)$, λ_j^{max} is the highest value of the range of variation, and λ_j^{min} is the lowest value. With regard to the range of variation allowed for the parameters, we must note that gradient routines work more efficiently if variations of similar magnitude on each of the search parameters introduce a similar variation on the function to minimize. The `E04FCF` user is advised to explore the region of parameters to minimize and to provide adequate rescaling of the problem before calling the routine. While the NAG library provides tools that help in this task, in our combined algorithm we take advantage of the knowledge obtained on the variation of the objective function during the previous evaluations performed by the GA. We use this exploration to normalize the χ^2 to unity and to rescale all the parameters affecting this function so that, according to the last evaluations of the best individuals explored by the GA, after rescaling of both the parameters and the function to optimize, the region explored by the NAG `E04FCF` routine in its search for the minima is expected to lie in a hypercube of unit volume. We have indeed verified that this normalization and rescaling procedure improves NAG routine performance.

Our minimization strategy includes the following aspects:

1. A first generation is made out of individuals randomly generated within reasonable values of the parameters.

2. Next, the GA is run for 400 *generations* (see definition further on). This number is determined af-

TABLE I: Ranges for the parameter values of the nucleon resonances. Masses and decay widths have been taken within the ranges provided by [22]. The helicity amplitudes are denoted by A^I_λ, where I stands for isospin and λ for the helicity of the initial photon-nucleon state.

	M^* (GeV)	Γ (GeV)	A^I_λ (GeV$^{-1/2}$)
$\Delta(1232)$	[1.215,1.219]	[0.094,0.098]	[-1,1]
N(1440)	[1.381,1.385]	[0.314,0.318]	[-1,1]
N(1520)	[1.502,1.506]	[0.110,0.114]	[-1,1]
N(1535)	[1.523,1.527]	[0.100,0.104]	[-1,1]
$\Delta(1620)$	[1.605,1.609]	[0.146,0.150]	[-1,1]
N(1650)	[1.661,1.665]	[0.238,0.242]	[-1,1]
$\Delta(1700)$	[1.724,1.728]	[0.116,0.120]	[-1,1]
N(1720)	[1.740,1.755]	[0.119,0.278]	[-1,1]

TABLE II: Ranges for the values of the parameters of vector mesons and cut-off Λ.

$F_{\omega NN}$	$[20.61, 21.11]$
K_ω	$[-0.17, -0.15]$
K_ρ	$[6.1, 6.3]$
Λ (GeV)	$[0.1, 2.0]$

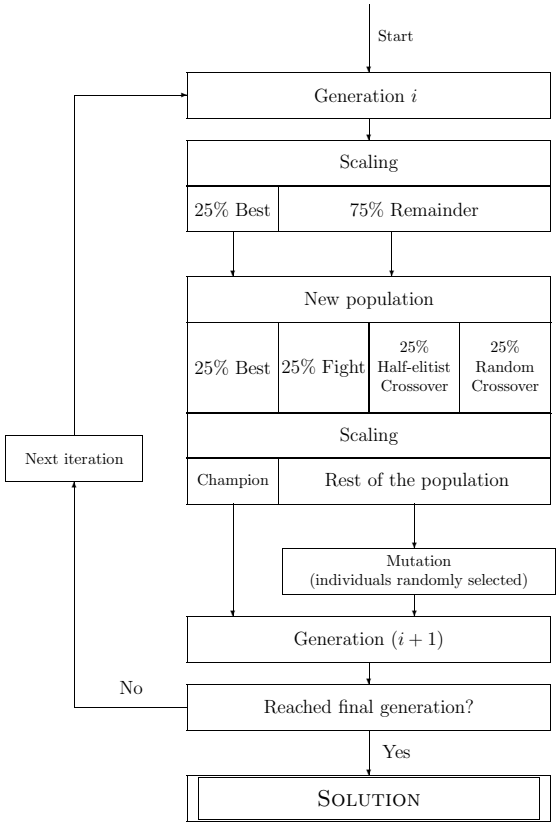

FIG. 2: GA scheme (see text in section IV).

ter inspecting the best individual evolution for each generation and from comparisons with benchmark problems of similar size. We do not really need that many as 400 generations (see Fig. 1), but we preferred to let the algorithm run for more generations than necessary in order to ensure that convergence was achieved.

3. After the 400 generations have been run, we introduce the GA solution as the initial value for the `E04FCF` routine from NAG libraries [9]. We use the routine for fine-tuning. The `E04FCF` routine implements an algorithm that looks for the unconstrained minimum of a sum of squares

$$\text{Minimize}\Big[F(x_1,\ldots,x_n)=\sum_{j=1}^{m}|f_j\,(x_1,\ldots,x_n)\,|^2\Big], \quad (6)$$

of m nonlinear functions in n variables ($m \geq n$). This algorithm does not require the derivatives to be known. From a starting point $x_1^{(1)}, \ldots, x_n^{(1)}$ (in our case supplied by the GA) the routine applies a Quasi-Newton method in order to find the minimum. This method uses a finite-difference approximation to the Hessian matrix to define the search direction. It is a very accurate and fast converging algorithm once we have an initial solution that is close to the minimum we seek. Therefore, it is well suited for our fine-tuning purpose.

We note that many attempts to solve our optimization procedure solely by means of `E04FCF` completely failed, even when we guided the initial ranges of the parameters by hand. The NAG routine got stuck in the first local minimum, usually very far from the one obtained by the GA.

4. We store the solution obtained by the combined algorithm and we start again, by generating a different random seed for the initial population of the GA. After running the minimization code twenty times, we obtain twenty different minima. If we find that all the χ^2 divided by χ^2_{min} (the minimum χ^2 among all the fits) are close to unity, we stop the fitting procedure.

IV. GENETIC ALGORITHM

Genetic Algorithms are a specific kind of stochastic optimization methods based upon the idea of evolution. There are many excellent textbooks on GA [18]. Here we will describe the main features of GA that are needed to understand our implementation. GAs encode the possible solutions to the proposed problem and deal with many of these solutions at the same time. Indeed, a set of these possible solutions (also called individuals or genes) form a population. Each individual in the population is classified according to its fitness value, computed

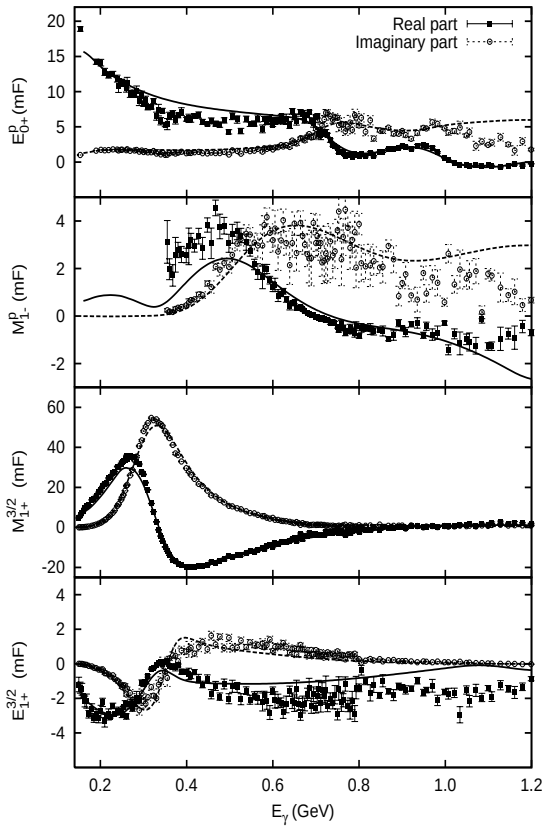

FIG. 3: Examples of the fits obtained to the electromagnetic multipoles for the reaction $\gamma p \to \pi^0 p$. Curve conventions: Solid: Real part of the electromagnetic multipole; Dashed: Imaginary part of the electromagnetic multipole. Data are from Ref. [6].

in terms of some objective function related to our optimization problem. In our case, the individual encodes the parameters of the Lagrangian and the objective function is essentially the χ^2 of the multipole values compared to the prediction of each Lagrangian represented in the population. GAs implement operators such as crossing among individuals and mutation [25]. As long as both the encoding of the problem and the GA operators exhibit good schema properties (that means that the offspring obtained after breeding two or more individuals with some good properties in terms of fitness are, more often than not, more fit than any of their parents), the *evolution* or repeated application of the genetic operators on the population, combined with a mechanism of natural selection (survival of the fittest), would cause some individuals to accumulate the good properties (subschema) initially distributed among different individuals in the early population. Provided that the number of individuals in the population is large enough for many good sub-schemas to be represented in at least some individual of the population, then the GAs would evolve toward very fit individuals, that is, good solutions to the problem. In this work, the obvious sub-schema are the parameters of each resonance and a simple encoding in which every individual is composed of a set of possible values for the parameters of our Lagrangian, would do the job. We encode the possible solutions to the problem (i.e., a complete set of parameters for the Lagrangian) as a series of integer numbers within the range from 0 to a maximum value N. For each parameter, this integer number represents the value of said parameter within the range desired by the user. For instance, a stored value of 0 would indicate that the value of the corresponding parameter equals the minimum allowed within the range. Conversely, the maximum value N would represent the stored parameter reaching the maximum allowed within the range. We denote this maximum value of these integers N as the *granularity* of our encoding strategy. A large value of N implies a very thin granularity, that is, relatively small changes in each parameter are possible in our encoding strategy and individuals that are very similar in terms of the parameters they represent and consequently, in their fitness, can be encoded. On the other hand, if we want to sample the parameter space with reasonable density, a too thin granularity would require a very large number of individuals. As we have just mentioned, an important choice to make for every GA is the number of individuals in the population. When the population size increases, the chances for relatively less fit individuals of mating with other individuals and generating better offspring before disappearing from the population, decrease exponentially. We must realize that even the less fit individuals (some of them) may have good sub-schema needed to encoded the best solution. Some of these sub-schema may not be present in other more fit individuals in the population, at least during the early stages of the evolution. According to results of tests with our Lagrangian as well as benchmarks with other functions that are easy to compute and have well known minima, we have determined that the maximum number of individuals we may safely employ in a population for our GA is around 400. For this size of the population, granularity values from 100 to 1000 have been employed in our GA without problems.

In what remains of this section we simply provide a detailed explanation on how the GA we have programed works. Our GA proceeds as follows 2:

1. Initial population. We provide a first *generation* consisting of individuals (400 in our calculations) that are randomly generated with reasonable values of the parameters [26].

2. Selection scheme. The genetic algorithm we use employs a scaled selection scheme and employs the elitist model [24]. In this model, the best individual (or champion) from the previous generation is always included in the current population, ensuring that the best solution this far is preserved. This decreases significantly the time the GA takes to find an acceptable solution. It has been proved [24] that

the GA which introduces elitism (that is, the guaranteed survival of the champion at every step of the GA evolution) will eventually converge to the absolute optimum, while, in general, the ones that do not protect the champion will never reach the optimum [27].

With regard to the remainder of the population, besides the champion, the individuals from the previous generation (that is, the population in its earlier state) are ranked according to the *fitness* function, in our case the χ^2 value. After this step, we introduce *scaling* of the population [28] determining the probability that an individual has to mate and survive. We provide a 0.8 probability to the worst individual and 1.0 to the best one. This is done in order to maintain genetic diversity. Indeed, it is necessary to prevent that the best and the worst individuals have a too different survival probability. If we do not take care to preserve genetic diversity in this way, the appearance of a very fit individual would make the forthcoming offspring collapse to the characteristics of that particularly fit individual too soon. Another important technique to maintain diversity is *mutation*, which is discussed further on.

3. After scaling, we classify the population into two sets. Set (a) is composed of the best 25% of the individuals and set (b) by the remaining 75%. We produce the new generation in the following way:

   - 25% of the individuals are taken from the most fit ones from the previous generation. That is, set (a) is copied into the next generation.
   - Another 25% is selected through a fight among all the individuals (tournament). The outcome of the fight is randomly decided, depending on probability. Even in the least favorable case (that is, if the worse individual fights with the best one), the winning probability of (the worst) individual is 15%. Winning probabilities are computed accordingly to the fitness of each contender.
   - Another 25% is obtained by means of half-elitist crossover. This means that we mate an individual from the best 25% of the previous generation (set (a)) with any other individual in sets (a) or (b). Both individuals are picked randomly from their respective sets.
   - The remaining 25% of the offspring are generated by mating individuals that are selected randomly without restrictions from sets (a) or (b).

   We apply two different kinds of crossover: *one point* crossover and *arithmetic* crossover [28]. In one point crossover, a random crossover point for both parents is selected. We split each chromosome from the parents into two pieces. We take the second piece of the second parent and attach it to the first piece of the first parent. In this way we obtain an individual that is a mixture of the two original ones. For the arithmetic crossover, we choose at random a number r between 0 and 1, and the offspring is calculated weighting the parents with weight r and $(1-r)$.

$$\lambda_i^{\text{offspring}} = r \cdot \lambda_i^{\text{parent 1}} + (1-r) \cdot \lambda_i^{\text{parent 2}} \qquad (7)$$

   Half of the crossovers our GA implements are one point and the other half are arithmetic. The kind of crossover to apply to a given pair of parents is chosen at random.

4. We evaluate the new population and identify the new champion. As previously mentioned, it will be preserved (elitism). We select other individuals to mutate from the rest of the population excluding the champion. Indeed, in each iteration of our GA we introduce as many mutations as the number of individuals in the population divided by three. These mutations are distributed at random among all the individuals (excluding the champion) of the population generated following the previous steps. We apply two types of mutation [29]. The *permutation* mutation exchanges two parameters selected at random. The *gaussian* mutation changes the value of a parameter by a small amount. The amount of change induced by this mutation is random within a small range. The reason to introduce mutations is that, quite often, the crossover operator and the selection method are too effective and they end up driving the GA toward a population of individuals that are almost exactly the same. When the population consists of similar individuals, the likelihood of finding new solutions typically decreases. The mutation operator introduces an additional randomness into the search. It helps to maintain diversity and to find solutions that crossover alone might not discover.

5. After these steps are taken, we say that a new generation is built. If we have not reached the limit in the number of generations, we run the algorithm again with the current set of individuals as the initial population.

   When the maximum number of generations has been reached, we take the set of parameters encoded by the champion as the solution given by GA to our problem. If sufficient generations have been run, most of the individuals will have close values for the fitness function.

It has been proven that there is no optimal algorithm that adapts well (that is, reaches a solution in the least number of evaluations) to all kind of problems. This is

TABLE III: Helicity amplitudes obtained in the fits in $\mathrm{GeV}^{-1/2}$.

	$A^p_{1/2}$	$A^\Delta_{1/2}$	$A^n_{1/2}$	$A^p_{3/2}$	$A^\Delta_{3/2}$	$A^n_{3/2}$
$\Delta(1232)$	–	−0.120	–	–	−0.229	–
N(1440)	0.060	–	−0.089	–	–	–
N(1520)	−0.007	–	0.032	0.107	–	−0.085
N(1535)	0.014	–	−0.137	–	–	–
$\Delta(1620)$	–	−0.023	–	–	–	–
N(1650)	−0.022	–	0.003	–	–	–
$\Delta(1700)$	–	0.139	–	–	−0.127	–
N(1720)	0.143	–	0.126	−0.004	–	−0.444

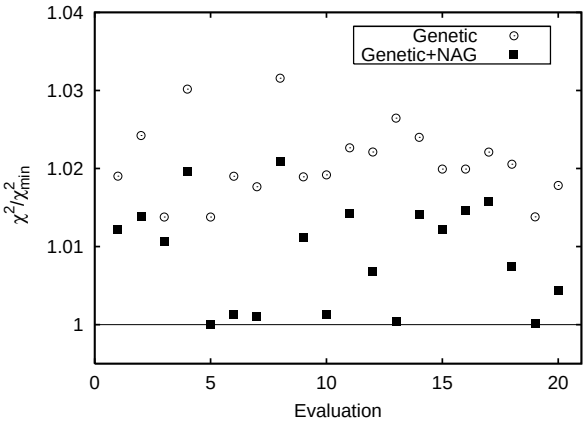

FIG. 4: Many local minima and the effect of the fine tuning performed by the `E04FCF` routine in the χ^2/χ^2_{min} are shown. Conventions: Open circles, χ^2/χ^2_{min} obtained by the GA alone (400 generations with 300 individuals each); Solid squares: χ^2/χ^2_{min} obtained by the GA plus the NAG routine.

often referred to as the *no free lunch theorem* in optimization [30]. Our goal here however is not to find the optimal algorithm that obtains the minimum to our problem in less evaluations but, rather, to develop a general tool that can be applied to many different models of parameter data fitting without specific fine-tuning nor human intervention, even if the performance of the tool is suboptimal in terms of the number of operations. In this regard, GAs are a handy choice, as they are suitable for many different problems. Thanks to scaling and elitism, our GA converges neither too quickly nor too slowly and generally it is able to find good candidates for the global optimum.

When the individuals are very fit, it can be hard for the GA to evolve further, mainly because the path to the best individual may involve two or more consecutive mutations where each of these mutations on their own will produce a less fit individual that will sooner be removed from the population. The occurrence of such two favorable mutations in the same individual is unlikely and tailored procedures must be implemented to introduce specific mutations that are adequate for particular problems, or more complex operators like the 'tunneling algorithm' [31] or complex rules to encode the values of the functions, like Mendelian operators implementing a non-dominant character for some genes [32]. In our work, however, we prefer to employ a hybrid optimization method that combines a standard hill-climbing algorithm with a GA. Hybrid optimization methods have been under study intensively [12, 33]. We have compared several ways of hybridizing GAs and conventional gradient based hill-climbing algorithms, such as introducing the hill-climbing algorithm as another mutation operator. However, we have noticed that this will only make the GA converge sooner, very often too soon, resulting in it getting stuck at any of the many local minima. From our experience, if the hill-climbing procedure is introduced just at the end of the evolution, when the GA has converged, the best results are achieved and a robust algorithm that requires no human intervention is this way configured. Also, no granularity is introduced in this final step of optimization. Indeed, the NAG routine is not restricted to integer values of the parameters, but instead represents each parameter as floating point values. Thus, we can also consider that the GA finds the best optimum that can be represented within the grid implied by the granularity N, and starting from this point of the grid, the NAG routine refines a search not bound to any grid values.

V. RESULTS

In Fig. 3 we show examples of fits to electromagnetic multipoles for the $\gamma p \to \pi^0 p$ process and the overall agreement obtained. The values of the parameters are summarized in Table III. In Fig. 1 we display an example of the evolution of the champion along the generations. Two hundred generations are sufficient enough to achieve convergence, but we run the algorithm for another two hundred generations to see the effects of mutations, which can reach areas of the parameter space that are not being fully surveyed by means of crossover.

We observe that at the early stages of the evolution the fitness function improves quickly, as crossover works to concentrate the good schema from other individuals into a good individual. Actually, a very steep slope in this region might indicate that evolution is too fast and that less fit individuals could disappear from the population before their good properties are transmitted to more fit individuals.

When a jump in the $\chi^2/\chi^2_{\rm min}$ happens, it is due to the appearance of a more fit new individual, either due to crossover or to mutation. In Fig. 4 we can verify the existence of many local minima (so this is certainly an ill-posed optimization problem) and the fine tuning achieved by the NAG routine which improves minima by approximately 2%.

An important issue to consider in GAs is efficiency. As we have already mentioned, the parameter space has

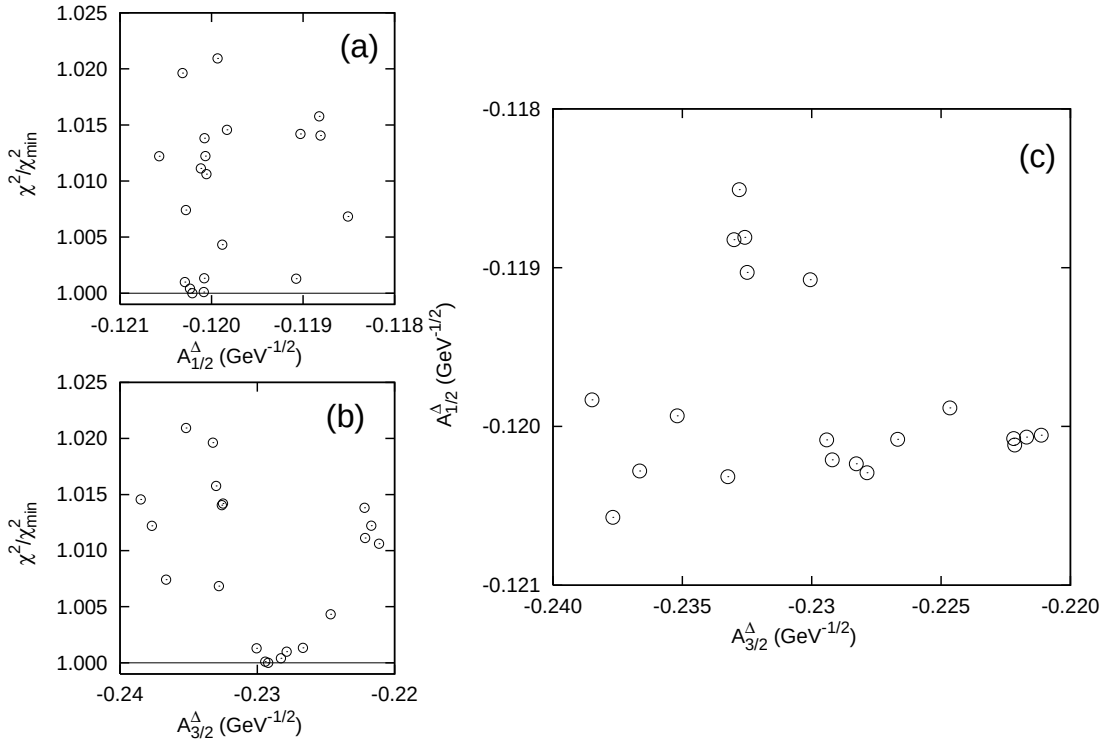

FIG. 5: Helicity amplitudes (equivalent to the coupling constants of the Lagrangians) of the $\Delta(1232)$. In all the figures we show the twenty minima obtained in the full minimization procedure (GA+NAG, see Fig. 4). The upper-left hand figure (a) shows the $\chi^2/\chi^2_{\rm min}$ versus the amplitude $A^{\Delta}_{1/2}$. The lower-left hand figure (b) shows the χ^2/χ^2min versus the amplitude $A^{\Delta}_{3/2}$. The right panel (c) shows $A^{\Delta}_{1/2}$ versus $A^{\Delta}_{3/2}$ parameters.

to be discretized with a certain granularity and the algorithm searches for the best solution within the discretized version of the parameter space. The size of this space significantly affects the efficiency of the algorithm, thus a balance between granularity and computing time has to be achieved. The gradient based routine allows us to gain precision and efficiency because we do not need the GA to reach the minimum, we simply need it to provide a value close enough for the `E04FCF` routine can reach it. In other words the GA has to reach the region where the minimum lies, and once in this region, reaching the minimum is a task for the gradient-based routine.

We must emphasize that the use of our algorithm is unattended. That is, we submit the script that starts 20 instances of the GA+NAG procedure, and after the equivalent to five CPU-days (Opteron, 2 GHz), we get the results for the optimized set of parameters. No further human intervention was needed to choose initial values of the parameters or to guide the evolution. While the GA+NAG may require more (costly) evaluations of the objective function, it is robust and needs no training nor good guesses of the initial parameters. Now that computer power seems to be an increasingly available resource, the unattended mode of operation makes this hybrid algorithm a very interesting alternative for these optimization problems.

Figs. 5 and 6 show a typical situation that may arise when the parameters are being determined. For $\Delta(1232)$ the minimum is well-established and all the minima are constrained in a small region. The size of the region where the minima lie may provide a better estimation of the error associated with the parameters than the one provided by the correlation matrix. On the other hand, in Fig. 5 the value for the $A^{\Delta}_{1/2}$ helicity amplitude appears to be in one of two split regions that are too close to be physically distinguished (left-upper panel). One region is centered at -0.120 and the other at -0.119 GeV$^{-1/2}$. The identification of these regions is one of the functionalities that GAs provide and one of their main advantages. When multiple regions containing minima of similar quality appear, the possible physical implications should be considered and further analysis to assess whether these different regions hold physical meaning (see subsection V A) is required.

We also show the minima of the $\Delta(1700)$ that are constrained in just one region. However, this region is larger than for the $\Delta(1232)$ and the experimental information available for this resonance, thus, yields parameters that are not as well established as for other nucleon excitations.

The evolution of the position of the parameters for different instances of the GA+NAG procedure as the number of generations employed in the GA increases, is shown for the $\Delta(1700)$ resonance in Figs. 7 and 8. We can ob-

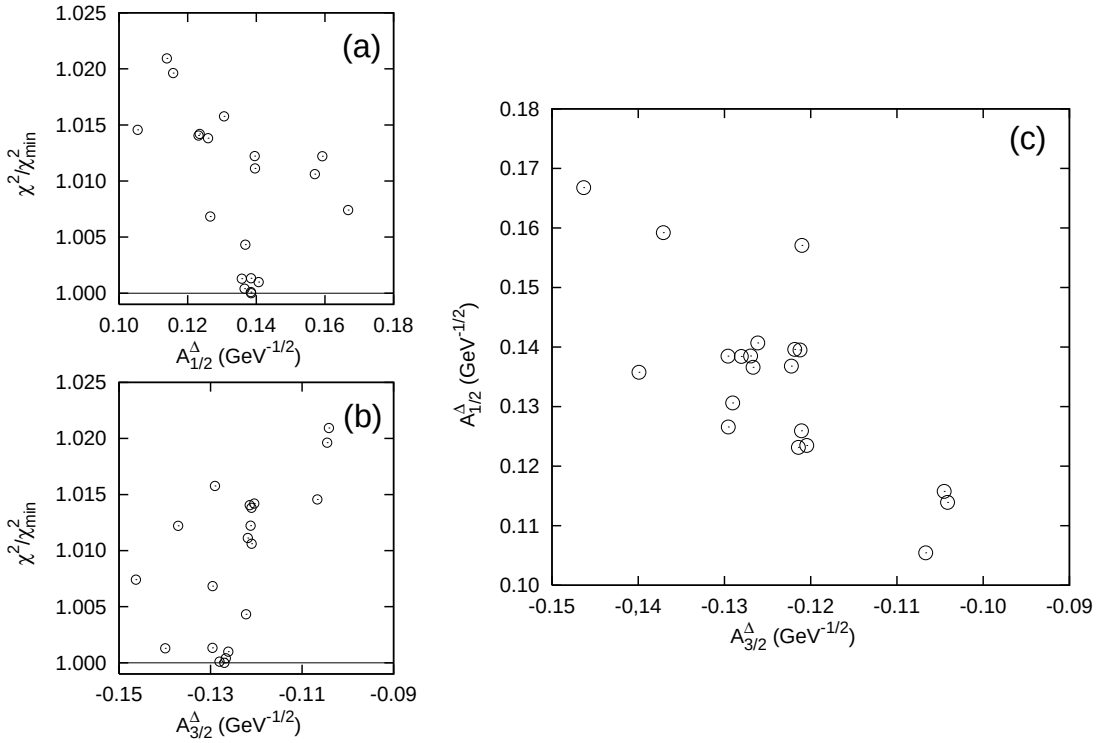

FIG. 6: Helicity amplitudes (equivalent to the coupling constants of the Lagrangians) of the $\Delta(1700)$. In all the figures we show the twenty minima obtained after the full minimization procedure (GA+NAG see Fig. 4). The upper-left hand figure (a) shows the $\chi^2/\chi^2_{\rm min}$ versus the amplitude $A^{\Delta}_{1/2}$. The lower-left hand figure (b) shows the $\chi^2/\chi^2_{\rm min}$ versus the amplitude $A^{\Delta}_{1/2}$. The right figure (c) shows $A^{\Delta}_{1/2}$ versus $A^{\Delta}_{3/2}$.

serve how the region of the minimum decreases while the GA evolves. For the 50 generations plus NAG run (asterisks in Figs. 7 and 8) the χ^2 is far away from its best value. This case exemplifies what happens when the parameters are assessed using the `E04FCF` after the GA had not been converged and therefore the GA is merely providing 'very smart guesses', for the starting point of the gradient based routine. We observe in this case that the results spread over a wide range of values of the parameters, showing that indeed this is a hard optimization problem. Indeed, we expect that the starting values provided by unconverged instances of the GA are in fact much better that the ones we may figure without the aid of the GA. It is clear that to reach even an average quality optimum would be extremely hard (if not impossible) without the GA phase of our algorithm. After 150 generations plus NAG (open squares in Figs. 7 and 8) the result looks much better, showing a region where the values of the parameters are well delimited. The χ^2 is remarkably better and close to the best values obtained after 400 generations plus NAG (solid circles in Figs. 6, 7, and 8).

A. Minima Split in Various Regions

The amount and quality of data is of great importance in assessing the parameters of any model. The pion photoproduction multipole data set employed for the fits in this work is the largest and of the highest quality ever available. It was released in 2006 and includes 3,760 data points. It is interesting to see what would happen if we employ the 2005 SAID database instead, which includes up to 1.0 GeV photon energy and considerably fewer (1526) data points, as done in Refs. [13, 14, 19]. We find that the results change for the not so well-determined resonances as is the case of the $\Delta(1700)$ one. We find in this case several minima lying in more than one region. Fig. 9 is equivalent to Fig. 6 but in this case fitting to the former data set. It becomes apparent how the minima split into two distinct regions. Fig. 10 is equivalent to Fig. 8 and shows how the regions are formed as the algorithm evolves. It also shows that a gradient method alone leads the optimization to incorrect answers most of the time. There are several possible reasons for the appearance of this minima structure. For instance, this can be caused by deficiencies in the model or in the data. We must keep in mind however, that this result can even have a physical meaning such as a possible shape coexistence for a state that can fit the data equally well for two sets of parameter values. This would have to be stud-

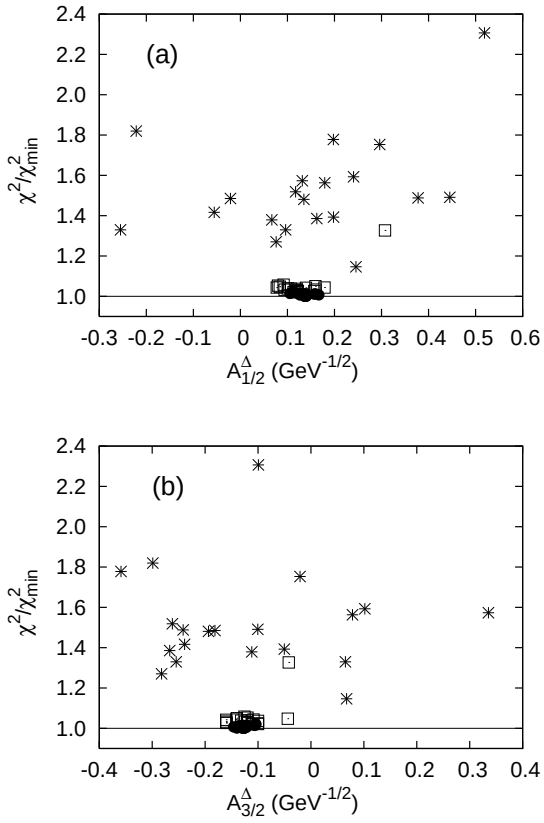

FIG. 7: Evolution of the minimization for the helicity amplitudes of the $\Delta(1700)$. Asterisks: minima obtained after 50 generations plus NAG; open squares: minima obtained after 150 generations plus NAG; solid circles: minima obtained after 400 generations plus NAG.

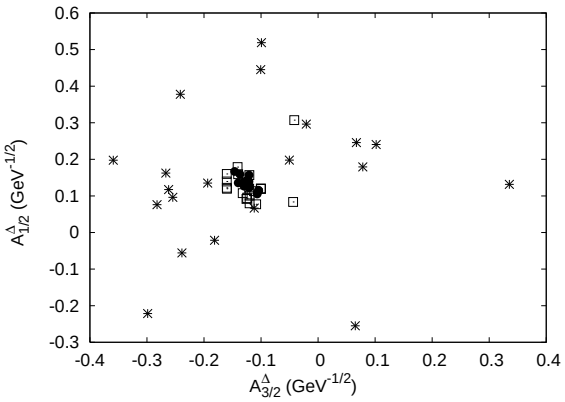

FIG. 8: Evolution of the minimization of the $\Delta(1700)$ helicity amplitudes. Same conventions as in Fig. 7.

ied within a model in which the resonance is included as a combination of both states and re-fit to experimental data. However, it seems that this is not the situation we encountered here. The results presented in the previous subsection and in Fig. 6 clearly indicate that improving the database and extending the model to higher energies (which allows one to account for the tail of the $\Delta(1700)$ resonance) are sufficient to collapse the two χ^2 regions into one single region.

VI. FINAL REMARKS

We have presented a hybrid optimization procedure which combines a GA with the gradient-based routine `E04FCF` from the NAG libraries. We have successfully applied this algorithm to determine the coupling constants of the low-lying nucleon resonances within a realistic Lagrangian model of the pion photoproduction reaction. The results for the couplings were summarized in Table III.

Traditional optimization tools are often useless for this kind of multi-parameter optimizations when the parameter space is large and the function to fit presents many local minima. The assessment of the low-lying resonances properties by means of reaction models is an example of a very difficult optimization problem for conventional algorithms [12, 13, 14].

The hybrid optimization procedure presented in this paper is a powerful and versatile optimization tool that can be applied to many problems in physics that involve the determination of a set of parameters from data. It is a promising method for extracting both reliable physical parameters as well as their confidence intervals. Indeed, computing correlations among different parameters by comparing different solutions obtained by the hybrid optimization method, in a manner similar to what is shown in the panel on the right in Fig. 6, is probably more meaningful than the simple covariance matrices returned by gradient based optimization routines.

Finally, we have shown how we can use the procedure we have outlined to identify weaknesses in the model and assess the reliability of the parameters obtained. Not only the error bars have to be considered when quoting the uncertainty in the determination of a parameter, but also whether the minima are concentrated into one single region or split into several ones, and the possible physical explanations of such situation.

Acknowledgments

This work has been supported in part under contracts FIS2005-00640, FPA2006-07393, and FPA2007-62216 of the Ministerio de Educación y Ciencia (Spain) and by UCM and the Comunidad de Madrid under project number 910059 (Grupo de Física Nuclear). C.F.-R. is supported by "Programa de becas posdoctorales" of the Ministerio de Educación y Ciencia (Spain). Part of the computations for this work were carried out at the "Cluster de Cálculo de Alta Capacidad para Técnicas Físicas", which is partly funded by the EU Commission under

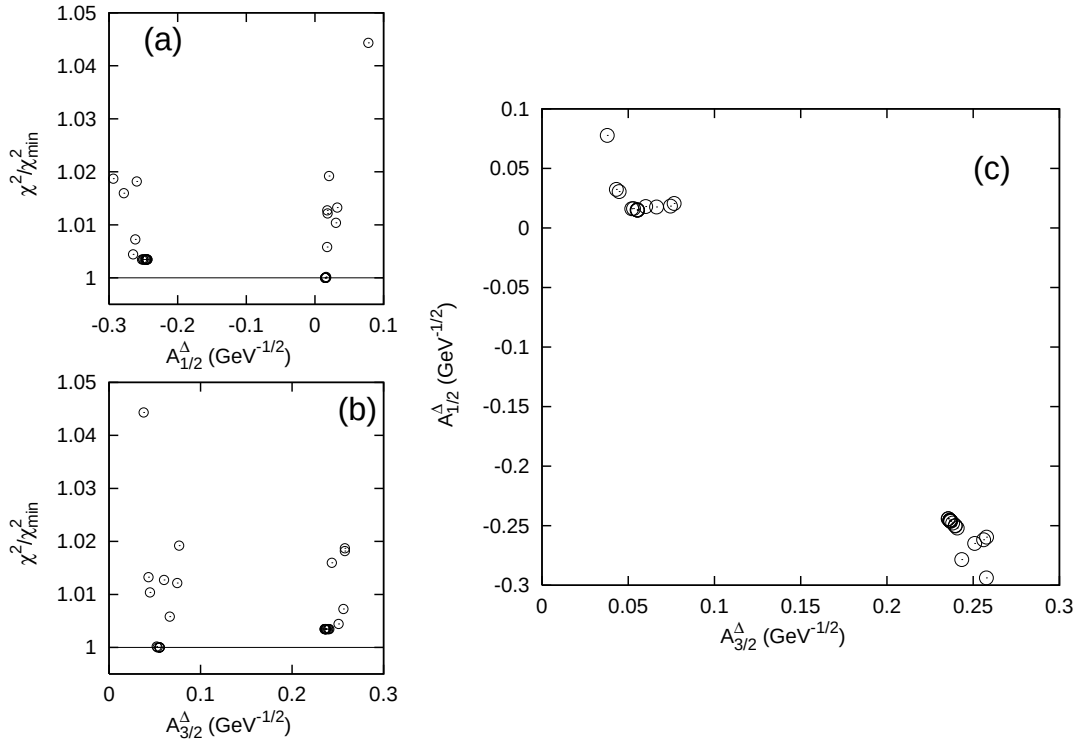

FIG. 9: Helicity amplitudes (equivalent to the coupling constants of the Lagrangians) of the $\Delta(1700)$. We show thirty minima obtained in the full minimization procedure (GA+NAG) for the 2005 SAID database up to 1 GeV of photon energy with the model in Ref. [14]. The upper hand left figure (a) shows the $\chi^2/\chi^2_{\rm min}$ versus the amplitude $A^{\Delta}_{1/2}$. The lower left hand figure (b) shows the $\chi^2/\chi^2_{\rm min}$ versus the amplitude $A^{\Delta}_{1/2}$. The figure on the right (c) shows $A^{\Delta}_{1/2}$ versus $A^{\Delta}_{3/2}$.

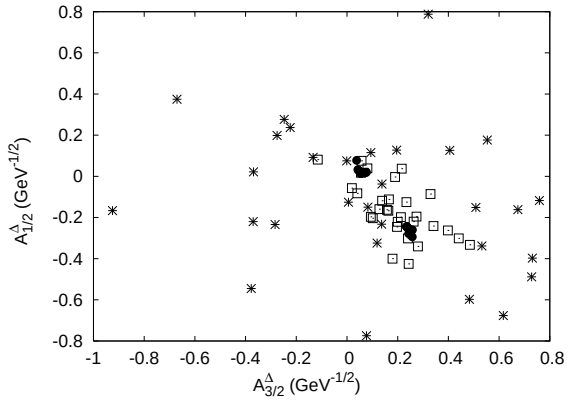

FIG. 10: Evolution of the minimization for the helicity amplitudes of the $\Delta(1700)$ for the 2005 SAID database. Asterisks: minima obtained after 50 generations plus NAG; open squares: minima obtained after 100 generations plus NAG; solid circles: minima obtained after 400 generations plus NAG. The formation of the two regions where the minima group can clearly be seen.

FEDER program and by the Universidad Complutense de Madrid (Spain).

[1] B. Krusche and S. Schadmand, Prog. Part. Nucl. Phys. **51**, 399 (2003).
[2] D.B. Leinweber, T. Draper, and R.M. Woloshyn, Phys. Rev. D **48**, 2230 (1993); C. Alexandrou, Ph. de Forcrand, H. Neff, J.W. Negele, W. Schroers, and A. Tsapalis, Phys. Rev. Lett. **94**, 021601 (2005).

[3] A. Wirzba and W. Weise, Phys. Lett. **B188**, 6 (1987).

[4] N. Isgur, G. Karl, and R. Koniuk, Phys. Rev. D **25**, 2394 (1982); A.J. Buchmann, E. Hernández, and A. Faessler, Phys. Rev. C **55**, 448 (1997); S. Capstick and W. Roberts, Prog. Part. Nucl. Phys. **45**, S241 (2000).

[5] C. Fernández-Ramírez and A. Relaño, Phys. Rev. Lett. **98**, 062001 (2007).

[6] R.A. Arndt, W.J. Briscoe, I.I. Strakovsky, and R.L. Workman, Phys. Rev. C **66**, 055213 (2002), SAID database, `http://gwdac.phys.gwu.edu`.

[7] G. Blanpied *et al.*, Phys. Rev. C **64**, 025203 (2001); A. Shafi *et al.*, Phys. Rev. C **70**, 035204 (2004).

[8] C. Molinari *et al.*, Phys. Lett. **B371**, 181 (1996); J. Peise *et al.*, Phys. Lett. **B384**, 37 (1996); R. Beck *et al.*, Phys. Rev. Lett. **78**, 606 (1997); F. Wissmann *et al.*, Nucl. Phys. **A660**, 232 (1999); B. Krusche *et al.*, Eur. Phys. J. **A22**, 277 (2004).

[9] Numerical Algorithms Group Ltd., Wilkinson House, Jordan Hill Road, Oxford OX2-8DR, UK, `http://www.nag.co.uk`.

[10] CERN, MINUIT 95.03, CERN Library D506 Edition, 1995.

[11] C. Winkler and H.M. Hofmann, Phys. Rev. C **55**, 684 (1997); I. Golovkin *et al.*, Phys. Rev. Lett. **88**, 045002 (2002); B.C. Allanach, D. Grellscheid, and F. Quevedo, J. High Energy Phys. JHEP07 (2004) 069.

[12] S. Janssen, D.G. Ireland, and J. Ryckebusch, Phys. Lett. **B562**, 51 (2003); D.G. Ireland, S. Janssen, and J. Ryckebusch, Nucl. Phys. **A740**, 147 (2004).

[13] C. Fernández-Ramírez, *Electromagnetic production of light mesons*, PhD dissertation, Universidad Complutense de Madrid (2006), `http://nuclear.fis.ucm.es/research/thesis/cesar_tesis.pdf`.

[14] C. Fernández-Ramírez, E. Moya de Guerra, and J.M. Udías, Ann. Phys. (N.Y.) **321**, 1408 (2006).

[15] C. Fernández-Ramírez, E. Moya de Guerra, and J.M. Udías, Phys. Lett. **B660**, 188 (2008).

[16] C. Fernández-Ramírez, E. Moya de Guerra, J.M. Udías, Phys. Lett. **B651**, 369 (2007).

[17] N. Metropolis, A.W. Rosenbluth, M.N. Rosenbluth, A.H. Teller, and E. Teller, J. Chem. Phys. **21**, 1087 (1953); S. Kirkpatrick, C. D. Gelatt, and M. P. Vecchi, Science **220**, 671(1983), `http://www.cs.virginia.edu/cs432/documents/sa-1983.pdf`; V. Cerny, J. Optim. Theory App. **45**, 41 (1985);.

[18] D.E. Goldberg, *Genetic Algorithms in Search, Optimization & Machine Learning* (Addison Wesley, Reading MA, 1989; L. Davis, *Handbook of Genetic Algorithms* (Van Nostrand Reinhold, New York NY, 1991); A.A. Törn and A. Zilinskas, *Global Optimization*, Lecture Notes in Computer Science 350 (Springer-Verlag, Berlin, 1989); M.D. Vose, *The Simple Genetic Algorithm* (MIT Press, Cambridge MA, 1999); Z. Michalewicz, *Genetic Algorithms+Data Structures=Evolution Programs* (Springer, Berlin-Heidelberg-New York, 1999); K. Deb, *Multi-Objective Optimization Using Evolutionary Algorithms* (Wiley, New York NY, 2002).

[19] C. Fernández-Ramírez, E. Moya de Guerra, and J.M. Udías, Phys. Rev. C **73**, 042201(R) (2006); Eur. Phys. J. **A31**, 572 (2007).

[20] W.-M. Yao *et al.*, J. Phys. **G33**, 1 (2006).

[21] V. Pascalutsa, Phys. Rev. D **58**, 096002 (1998); V. Pascalutsa and R. Timmermans, Phys. Rev. C **60**, 042201(R) (1999).

[22] T.P. Vrana, S.A. Dytman, and T.-S.H. Lee, Phys. Rep. **328**, 181 (2000).

[23] R.M. Davidson and R. Workman, Phys. Rev. C **63**, 058201 (2001); Phys. Rev. C **63**, 025210 (2001).

[24] K. A. De Jong, *An analysis of the behavior of a class of genetic adaptive systems*, PhD dissertation, University of Michigan (1975).

[25] L.J. Eshelman and D.J. Shaffer, *Preventing premature convergence in genetic algorithms by preventing incest*, in L.B. Belew and R.K. Booker (Eds.), Proceedings of the 4th International Conference on Genetic Algorithms, p. 115 (Morgan Kaufmann, San Diego CA, 1991); T. Bäck, *Optimal mutation rates in genetic search*, in S. Forrest (Ed.), Proceedings of the 5th International Conference on Genetic Algorithms, p. 2 (Morgan Kaufmann, San Mateo CA, 1993).

[26] D.E. Goldberg, *Optimal initial population size for binary coded genetic algorithms* (TCGA Technical report 85001) Tuscaloosa: University of Alabama, The Clearinghouse for Genetic Algorithms (1985); D.E. Goldberg, K. Deb, and J.H. Clark, Complex Systems **6**, 333 (1992).

[27] G. Rudolph, IEEE Trans. Neural Netw. **5**, 96 (1994).

[28] D.E. Goldberg and K. Deb, *A comparative analysis of selection schemes used in genetic algorithms*, in G.J.E. Rawlins (ed.), Foundations of Genetic Algorithms, p. 69 (Morgan Kaufmann, San Mateo CA, 1991).

[29] W.M. Spears, *Evolutionary algorithms: The role of mutation and recombination* (Springer, Berlin-Heidelberg, 2004).

[30] D.H. Wolpert and W.G. Macready, IEEE Trans. Evol. Comput. **1**, 67 (1997), `http://ic.arc.nasa.gov/people/dhw/papers/78.pdf`.

[31] A.V.Levy and A. Montalvo, SIAM J. Sci. Stat. Comput. **6**, 15 (1985).

[32] I.-S. Song, H.-W. Woo, and M.J. Tahk, *A genetic algorithm with a mendel operator for global minimization*, in Proceedings of the 1999 Congress on Evolutionary Computation CEC99, Vol. 2, p. 1526, `http://ieeexplore.ieee.org/iel5/6342/16979/00782664.pdf?tp=`

[33] J.-M. Renders and S.P. Flasse, IEEE Trans. Syst. Man Cybern. Part B-Cybern. **26**, 243 (1996). D. Quagliarella and A. Vicini, *Hybrid genetic algorithms as tools for complex optimisation problems*, in P. Blonda, M. Castellano, and A. Petrosino (eds.), New Trends in Fuzzy Logic II. Proceedings of the Second Italian Workshop on Fuzzy Logic, p. 300, (World Scientific, Singapore, 1998); D.E. Goldberg and S. Voessner, *Optimizing global-local search hybrids*, in W. Banzhaf, J. Daida, A.E. Eiben, M.H. Garzon, V. Honavar, M. Jakiela, and R.E. Smith (eds.), Proceedings of the Genetic and Evolutionary Computation Conference, p. 220 (Morgan Kaufmann, San Francisco CA, 1999);